TABLE 1. Semi-quantification of Cx37 expression in afferent arterioles

	Control	Diabetes
WT	2.0 ± 0.45 (5)	1.8 ± 0.31 (6)
eNOS Tg	2.2 ± 0.31 (6)	2.5 ± 0.50 (4)
eNOS KO	1.5 ± 0.22 (6)	1.3 ± 0.21 (6)

No significant differences amongst wild type (WT), eNOS transgenic (Tg) and eNOS knockout (KO) mice and their diabetic counterparts ($p > 0.05$). The numbers in parentheses represent the number of animals studied.

TABLE 2. Semi-quantification of Cx40 expression in afferent arterioles

	Control	Diabetes
WT	1.6 ± 0.40 (5)	3.0 ± 0.32 (5)*
eNOS Tg	2.3 ± 0.25 (4)#	4.0 ± 0.00 (4)†
eNOS KO	1.0 ± 0.00 (4)	1.5 ± 0.50 (4)

#$p < 0.05$ compared to eNOS knockout control mice; *$p < 0.05$ compared to wild type control mice.
†$p < 0.05$ compared to eNOS Tg control mice. Numbers in parentheses represent the number of animals studied. KO: knockout. WT: wild type, Tg: transgenic; KO: knockout.

In wild-type mice, expression of Cx40 was more restricted to the smooth muscle cells immediately adjacent to the renin-secreting cells (Fig. 2A), while in the corresponding areas in eNOS knockout mice, Cx40 was either similar to or weaker than that in the wild-type mice (Fig. 2E). In contrast, clear and consistent Cx40 staining in the smooth muscle cells beyond the renin-secreting cells was detected in eNOS transgenic mice (Fig. 2C). Semiquantification of Cx40 staining showed a significant increase in Cx expression in the afferent arterioles of eNOS transgenic mice compared to that in eNOS knockout mice ($P < 0.05$; Table 2, control). No significant difference in Cx staining was observed between wild-type and eNOS transgenic mice or wild-type and eNOS knockout mice.

Cx43 was detected in endothelial cells of afferent arterioles from wild-type, eNOS transgenic, and eNOS knockout mice (Fig. 3A, C, and E). Cx43 was not detected in smooth muscle cells of afferent arterioles in any of the three groups.

Diabetic mice. Since the previous sections indicated that overexpression of eNOS mimicked changes of Cxs seen previously in diabetes (Zhang and Hill, 2005), we tested this hypothesis by inducing diabetes in eNOS knockout mice.

Expression of Cx37 and Cx40 in endothelial cells and renin-secreting cells of afferent arterioles was similar among wild-type, eNOS transgenic, and eNOS knockout diabetic mice (Figs. 1B, D, and F and 2B, D, and F).

In the smooth muscle cells, expression of Cx37 was also similar among wild-type, eNOS transgenic, and eNOS knockout diabetic mice (Fig. 1B, D, and F). No statistically significant difference was detected between control mice and their counterpart diabetic mice, although there was a tendency for reduced expression in eNOS knockout mice ($P > 0.05$; Table 1).

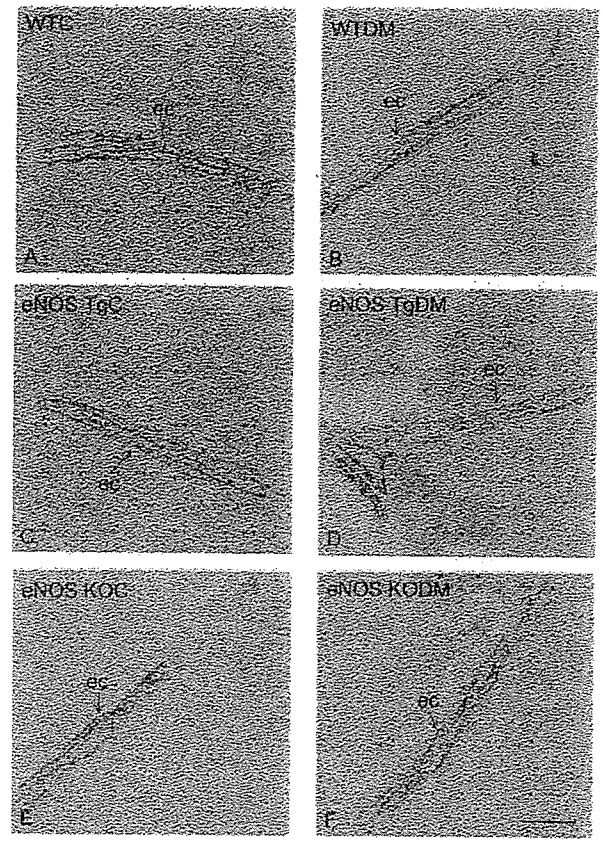

Fig. 3. Expression of Cx43 in afferent arterioles. Cx43 was detected in endothelial cells (ec) in wild-type control (WTC, **A**) and diabetic mice (WTDM, **B**), eNOS transgenic control (eNOS TgC, **C**) and diabetic mice (eNOS TgDM, **D**), eNOS knockout control (eNOS KOC, **E**), and diabetic mice (eNOS KODM, **F**). No staining was detected in the smooth muscle cells. The vessels were oriented longitudinally from left to right. Scale bar = 20 μm.

Expression of Cx40 was increased in the distal smooth muscle cells of afferent arterioles of both wild-type diabetic mice and eNOS transgenic diabetic mice, the staining being more consistent in eNOS transgenic mice than that in wild-type mice (Fig. 2A–D). In eNOS knockout diabetic mice, Cx40 staining was restricted to the smooth muscle cells immediately adjacent renin-secreting cells (Fig. 2F). Semiquantification of Cx40 in smooth muscle cells showed a significant increase in Cx staining in wild-type diabetic mice compared to wild-type control and in eNOS transgenic diabetic mice compared to eNOS transgenic control mice ($P < 0.05$; Table 2). No significant difference was detected in Cx staining between eNOS knockout diabetic mice and eNOS knockout control mice ($P > 0.05$; Table 2). However, expression of Cx40 in afferent arterioles of eNOS knockout diabetic mice was significantly less than that in afferent arterioles of wild-type diabetic or eNOS transgenic diabetic mice ($P < 0.05$).

Cx43 was detected in endothelial cells of afferent arterioles from all diabetic groups in a similar manner to

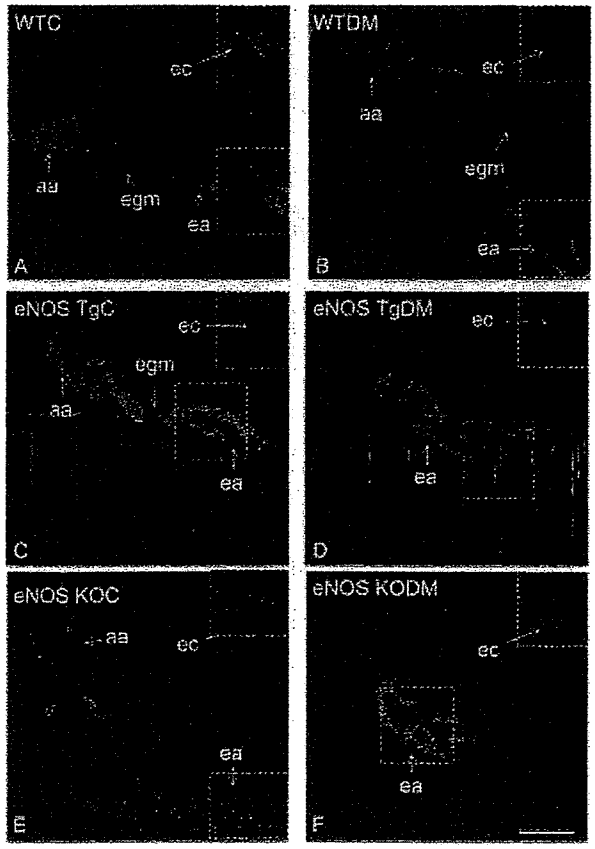

Fig. 4. Expression of Cx43 in efferent arterioles. When arterioles were labeled with antimyosin staining, Cx43 was detected in endothelial cells (ec) of the efferent arterioles (ea) in wild-type (WTC, **A**) and eNOS knockout control mice (eNOS KOC, **E**), but it was not detected in eNOS transgenic control mice (eNOS TgC, **C**). In diabetes, Cx43 staining was reduced in wild-type diabetic (WTDM, **B**), while it was unchanged in eNOS knockout diabetic mice (eNOS KODM, **F**). Cx43 was not detected in eNOS transgenic diabetic mice (eNOS TgDM, **D**). Cx43 was not detected in extraglomerular mesangial cells (egm) in all groups. The insets show Cx43 staining in the same field as the box but without double labeling with antimyosin. Afferent arterioles (aa) were oriented on the left (A, B, C, E). Scale bar = 20 μm.

that in the control groups (Fig. 3). Cx43 was not detected in the smooth muscle cells of any diabetic mice (Fig. 3B, D, and F).

Connexin Expression in Efferent Arterioles

Nondiabetic mice. Only Cx43 was detected in endothelial cells of efferent arterioles from wild-type mice (Fig. 4A), as we have reported previously (Zhang and Hill, 2005). In contrast, Cx43 was not found in endothelial cells of efferent arterioles in eNOS transgenic mice (Fig. 4C) but was detected strongly in endothelial cells of efferent arterioles in eNOS knockout mice (Fig. 4E). Semiquantification of Cx staining showed a significant decrease in Cx expression in endothelial cells of efferent arterioles in eNOS transgenic mice compared to that in wild-type control mice or in eNOS knockout control mice ($P < 0.05$; Table 3, control). However, no difference was detected between wild-type control and eNOS knockout control mice ($P > 0.05$; Table 3, control). Neither Cxs37, 40 (not shown), nor Cx43 was detected in the smooth muscle cells of efferent arterioles in any of the three groups (Fig. 4A, C, and E).

TABLE 3. Semi-quantification of Cx43 in efferent arterioles

	Control	Diabetes
WT	2.2 ± 0.20 (5)	1.4 ± 0.25 (5)*
eNOS Tg	1.0 ± 0.00 (4)†	1.0 ± 0.00 (4)
eNOS KO	2.8 ± 0.25 (4)	2.8 ± 0.25 (4)

†$p < 0.05$ compared to wild type (WT) control and eNOS knockout (KO) control mice.
*$p < 0.05$ compared to wild type control mice. The numbers in the parentheses represent the number of animals studied. Tg: transgenic.

Diabetic mice. During diabetes, Cxs37 and 40 remained absent from endothelial cells of efferent arterioles in wild-type, eNOS transgenic, and knockout mice. Expression of Cx43 in endothelial cells of efferent arterioles was reduced in wild-type diabetic mice compared to that in wild-type control mice (Fig. 4A and B). No Cx43 was detected in eNOS transgenic diabetic mice (Fig. 4D), while Cx43 was readily detected in endothelial cells of efferent arterioles in eNOS knockout diabetic mice (Fig. 4F). Semiquantification of Cx staining showed a significant decrease in Cx43 in wild-type diabetic mice compared to that in wild-type control mice ($P < 0.05$; Table 3), consistent with our previous results (Zhang and Hill, 2005). No significant difference was detected between eNOS transgenic control and diabetic mice or between eNOS knockout control and diabetic mice ($P > 0.05$; Table 3). Expression of Cx43 was significantly greater in efferent arterioles of eNOS knockout diabetic mice than in efferent arterioles of wild-type diabetic or eNOS transgenic diabetic mice ($P < 0.05$). No Cxs were detected in the smooth muscle cells of efferent arterioles in any of the diabetic groups.

Expression of eNOS Protein in Normal and Diabetic Mice

eNOS was expressed in endothelial cells of large and small arteries in wild-type mice (Fig. 5A). In eNOS transgenic mice, staining for eNOS was markedly stronger but still confined to the endothelium of the vascular wall (Fig. 5B). eNOS expression was absent from the endothelium of the vascular wall in eNOS knockout mice (Fig. 5C).

During diabetes, the intensity of eNOS fluorescence in the endothelium of afferent arterioles was markedly increased in wild-type diabetic mice (Fig. 5D) compared to that in wild-type control mice (Fig. 5A). eNOS expression in eNOS transgenic diabetic mice (Fig. 5E) was similar to or weaker than that in eNOS transgenic control mice (Fig. 5B). eNOS expression was absent from the endothelium of the eNOS knockout diabetic mice.

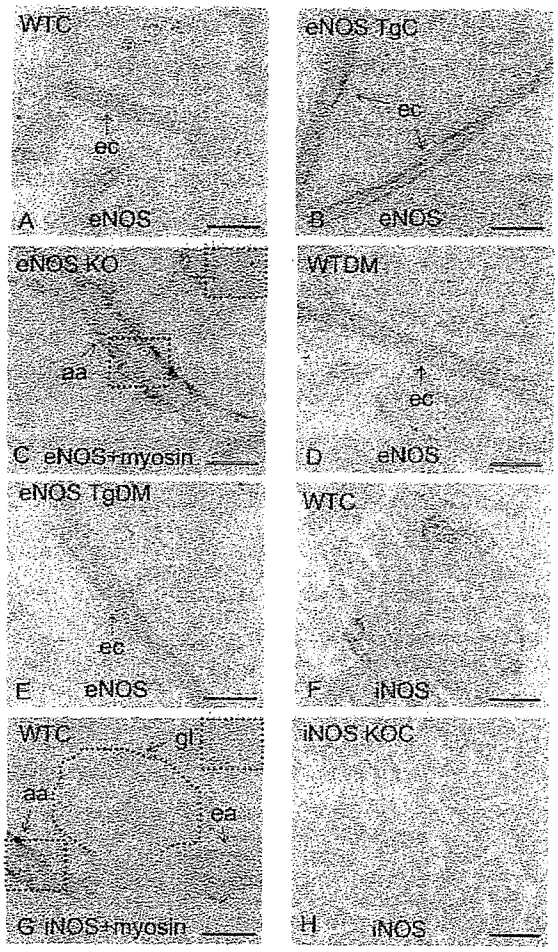

Fig. 5. Expression of eNOS and iNOS protein. eNOS was detected in endothelial cells of afferent arterioles (aa) in wild-type control (WTC, **A**) and diabetic mice (WTDM, **D**), eNOS transgenic control (eNOS TgC, **B**) and diabetic mice (eNOS TgDM, **E**). eNOS protein was not detected in eNOS knockout control mice when double-labeled with antimyosin staining (eNOS KOC, **C**). iNOS expression was not detected in smooth muscle cells of afferent arterioles (aa) or efferent arterioles (ea) in wild-type control mice when double-labeled with antimyosin staining (WTC, **G**), nor was iNOS detected inside the glomerulus (WTC, G). iNOS protein was detected in renal tubules in wild-type control mice (WTC, **F**) but not in iNOS knockout mice (iNOS KOC, **H**). The insets showed anti-eNOS (C) or anti-iNOS (G) staining in the same field as the box but without double labeling with antimyosin. gl, glomerulus. Scale bars = 20 μm in A–D, E and G; 50 μm in F and H.

Expression of iNOS Protein in Juxtaglomerular Apparatus

iNOS protein expression was mainly detected in the tubules located in the medulla and occasionally in some tubules in the cortex of wild-type and eNOS transgenic mice (Fig. 5F). iNOS protein was not expressed in the afferent or efferent arterioles when double-labeled with antimyosin staining (Fig. 5G) in any of the mice groups under normal or diabetic conditions. The specificity of iNOS antibody was confirmed by lack of iNOS staining in tubules within the renal medulla of iNOS knockout mice (Fig. 5H).

DISCUSSION

Our study has shown that in eNOS transgenic mice, Cx40 was well expressed in smooth muscle cells of afferent arterioles, while Cx43 was absent from endothelial cells of efferent arterioles. This pattern is similar to that observed in wild-type mice during diabetes (Zhang and Hill, 2005). In contrast, expression levels of Cxs40 and 43 in afferent and efferent arterioles of eNOS knockout mice were similar to those of wild-type mice. Furthermore, induction of diabetes in eNOS knockout mice failed to produce any changes in Cx expression in either afferent or efferent arterioles, suggesting that changes in Cx expression associated with diabetes correlate with an increase in eNOS expression. Immunohistochemistry confirmed that eNOS was upregulated in endothelial cells of wild-type mice during diabetes and in eNOS transgenic mice but was absent from eNOS knockout mice. The effect on Cx expression was not due to compensatory changes in iNOS since expression of iNOS was not detected in either afferent arterioles or efferent arterioles in any of the mice groups.

Our data suggest that overexpression of eNOS during diabetes produces completely different changes in Cxs in afferent and efferent arterioles. This differential responsiveness is consistent with numerous studies that have shown differences in structure and function of these two arterioles. Thus, the vascular wall of afferent arterioles is thick and composed of uniformly distributed smooth muscle cells, while the vascular wall of efferent arterioles in the superficial cortex is thin, irregular, and composed of irregularly shaped smooth muscle cells (Evan and Dail, 1977; Gattone et al., 1984; Bankir et al., 1987; Yuan et al., 1990). This morphological heterogeneity of renal arterioles was confirmed by antimyosin staining in the present study and was one of the criteria used to differentiate afferent arterioles from efferent arterioles. Furthermore, myosin heavy chain-B isoform is predominantly expressed in afferent arterioles, whereas myosin heavy chain-A isoform is only expressed in the efferent arterioles (Shiraishi et al., 2003). From a functional standpoint, differences also exist. Thus, afferent arterioles express both angiotensin type 1A and type 1B receptors while efferent arterioles exclusively express type 1A receptors (Harrison-Bernard et al., 2006). Furthermore, contractile responses in afferent arterioles are more dominated by voltage-dependent ion channels than those of efferent arterioles (Carmines and Navar, 1989; Loutzenhiser and Loutzenhiser, 2000; Hansen et al., 2001). Differential remodeling of afferent and efferent arterioles during diabetes has also been reported in streptozotocin-treated diabetic rats (Turoni et al., 2005).

The nature of the changes in Cx expression in afferent versus efferent arterioles suggests that eNOS overexpression accentuates the limited coupling between preglomerular vasculature and postglomerular vasculature. This accentuation might further aggravate glomerular hyperfiltration in the early stage of diabetes (Carmines and Fujiwara, 2002). Increased Cx expression within the preglomerular smooth muscle might also enhance the differential neural control of afferent and efferent arterioles, leading to increased pressure drop across the glo-

merulus (Denton et al., 2004), further precipitating glomerular hyperfiltration.

Increased expression of eNOS has been shown previously in the aorta (Asaba et al., 2005) and glomeruli of diabetic rats (Satoh et al., 2005). However, the increased eNOS expression in the latter study was accounted for by monomeric eNOS, rather than the functional dimeric eNOS, which was decreased. Thus, these changes in eNOS resulted in reduced generation of NO (Satoh et al., 2005) and increased production of reactive oxygen species (ROS) due to eNOS uncoupling (Satoh et al., 2005; Bevers et al., 2006). Since ROS and high glucose are also NO scavengers, the bioavailability of NO during diabetes is further reduced, as found in the renal cortex of diabetic rats (Palm et al., 2005). On the other hand, increased eNOS expression in eNOS transgenic mice results in increased production of NO as demonstrated in the aorta (Yamashita et al., 2000). Therefore, although the Cx changes in diabetes are similar to those observed in eNOS transgenic mice, the effect cannot be simply attributed to increased production of endothelial NO. In spite of these differences, changes to one of the downstream effectors of NO appear to be similar in diabetic and eNOS transgenic animals. Thus, although cGMP levels were increased in eNOS transgenic mice, NO-induced vasorelaxation was reduced due to decreased activity of both guanylate cyclase and protein kinase G (Yamashita et al., 2000). A similar decrease in NO-induced vasorelaxation has been reported in aorta of streptozotocin-induced diabetic rats due to decrease in guanylate cyclase and protein kinase G-protein (Zanetti et al., 2005). Interestingly, the activity of guanylate cyclase was increased in eNOS knockout mice (Brandes et al., 2000). Further experimentation is therefore necessary to clarify the involvement of guanylate cyclase and ROS in the mechanism by which elevated eNOS protein can alter Cx expression.

Together, our data demonstrate that an increase in eNOS protein can produce significant changes in expression of Cxs40 and 43 in afferent and efferent arterioles. These changes mimic those occurring in diabetes, during which eNOS protein is similarly increased in these arterioles. The regulation by eNOS of vascular Cx expression differs between the afferent and efferent arterioles in relation to both the cell type and Cx subtype involved, providing further evidence of the appreciable differences in structure and function of these two renal vessels.

ACKNOWLEDGMENTS

The authors thank Dr. Klaus Matthaei for designing the primers for eNOS transgenic genotyping and Mrs. Kate Meaney for assistance with the quantification of the immunohistochemical data.

LITERATURE CITED

Asaba K, Tojo A, Onozato ML, Goto A, Quinn MT, Fujita T, Wilcox CS. 2005. Effects of NADPH oxidase inhibitor in diabetic nephropathy. Kidney Int 67:1890–1898.

Bankir L, Bouby N, Trinh-Trang-Tan MM. 1987. Heterogeneity of nephron anatomy. Kidney Int 20(Suppl):S25–S39.

Bevers LM, Braam B, Post JA, van Zonneveld AJ, Rabelink TJ, Koomans HA, Verhaar MC, Joles JA. 2006. Tetrahydrobiopterin, but not L-arginine, decreases NO synthase uncoupling in cells expressing high levels of endothelial NO synthase. Hypertension 47:87–94.

Brandes RP, Kim D, Schmitz-Winnenthal FH, Amidi M, Godecke A, Mulsch A, Busse R. 2000. Increased nitrovasodilator sensitivity in endothelial nitric oxide synthase knockout mice: role of soluble guanylyl cyclase. Hypertension 35:231–236.

Carmines PK, Navar LG. 1989. Disparate effects of Ca channel blockade on afferent and efferent arteriolar responses to ANG II. Am J Physiol 256:F1015–F1020.

Carmines PK, Fujiwara K. 2002. Altered electromechanical coupling in the renal microvasculature during the early stage of diabetes mellitus. Clin Exp Pharmacol Physiol 29:143–148.

Christ GJ, Spray DC, el-Sabban M, Moore LK, Brink PR. 1996. Gap junctions in vascular tissues: evaluating the role of intercellular communication in the modulation of vasomotor tone. Circ Res 79: 631–646.

Denton KM, Luff SE, Shweta A, Anderson WP. 2004. Differential neural control of glomerular ultrafiltration. Clin Exp Pharmacol Physiol 31:380–386.

Evan AP, Dail WG Jr. 1977. Efferent arterioles in the cortex of the rat kidney. Anat Rec 187:135–145.

Gattone VH II, Luft FC, Evan AP. 1984. Renal afferent and efferent arterioles of the rabbit. Am J Physiol 247:F219–F228.

Hansen PB, Jensen BL, Andreasen D, Skott O. 2001. Differential expression of T- and L-type voltage-dependent calcium channels in renal resistance vessels. Circ Res 89:630–638.

Harats D, Kurihara H, Belloni P, Oakley H, Ziober A, Ackley D, Cain G, Kurihara Y, Lawn R, Sigal E. 1995. Targeting gene expression to the vascular wall in transgenic mice using the murine preproendothelin-1 promoter. J Clin Invest 95:1335–1344.

Harris AL. 2001. Emerging issues of connexin channels: biophysics fills the gap. Q Rev Biophys 34:325–472.

Harrison-Bernard LM, Monjure CJ, Bivona BJ. 2006. Efferent arterioles exclusively express the subtype 1A angiotensin receptor: functional insights from genetic mouse models. Am J Physiol 290: F1177–F1186.

Hill CE, Phillips JK, Sandow SL. 2001. Heterogeneous control of blood flow amongst different vascular beds. Med Res Rev 21:1–60.

Hill CE, Rummery N, Hickey H, Sandow SL. 2002. Heterogeneity in the distribution of vascular gap junctions and connexins: implications for function. Clin Exp Pharmacol Physiol 29:620–625.

Hoffmann A, Gloe T, Pohl U, Zahler S. 2003. Nitric oxide enhances de novo formation of endothelial gap junctions. Cardiovasc Res 60: 421–430.

Huang PL, Huang Z, Mashimo H, Bloch KD, Moskowitz MA, Bevan JA, Fishman MC. 1995. Hypertension in mice lacking the gene for endothelial nitric oxide synthase. Nature 377:239–242.

Kawashima S, Yamashita T, Ozaki M, Ohashi Y, Azumi H, Inoue N, Hirata K, Hayashi Y, Itoh H, Yokoyama M. 2001. Endothelial NO synthase overexpression inhibits lesion formation in mouse model of vascular remodeling. Arterioscler Thromb Vasc Biol 21:201–207.

Kuroki T, Inoguchi T, Umeda F, Ueda F, Nawata H. 1998. High glucose induces alteration of gap junction permeability and phosphorylation of connexin-43 in cultured aortic smooth muscle cells. Diabetes 47:931–936.

Loutzenhiser K, Loutzenhiser R. 2000. Angiotensin II-induced Ca(2+) influx in renal afferent and efferent arterioles: differing roles of voltage-gated and store-operated Ca(2+) entry. Circ Res 87:551–557.

Ohashi Y, Kawashima S, Hirata K, Yamashita T, Ishida T, Inoue N, Sakoda T, Kurihara H, Yazaki Y, Yokoyama M. 1998. Hypotension and reduced nitric oxide-elicited vasorelaxation in transgenic mice overexpressing endothelial nitric oxide synthase. J Clin Invest 102: 2061–2071.

Ozaki M, Kawashima S, Hirase T, Yamashita T, Namiki M, Inoue N, Hirata Ki K, Yokoyama M. 2002. Overexpression of endothelial nitric oxide synthase in endothelial cells is protective against ischemia-reperfusion injury in mouse skeletal muscle. Am J Pathol 160: 1335–1344.

Paik SG, Fleischer N, Shin SI. 1980. Insulin-dependent diabetes mellitus induced by subdiabetogenic doses of streptozotocin: oblig-

atory role of cell-mediated autoimmune processes. Proc Natl Acad Sci USA 77:6129–6133.

Palm F, Buerk DG, Carlsson PO, Hansell P, Liss P. 2005. Reduced nitric oxide concentration in the renal cortex of streptozotocin-induced diabetic rats: effects on renal oxygenation and microcirculation. Diabetes 54:3282–3287.

Prabhakar SS. 2004. Role of nitric oxide in diabetic nephropathy. Semin Nephrol 24:333–344.

Roh CR, Heo JH, Yang SH, Bae DS. 2002. Regulation of connexin 43 by nitric oxide in primary uterine myocytes from term pregnant women. Am J Obstet Gynecol 187:434–440.

Rummery NM, Hickey H, McGurk G, Hill CE. 2002. Connexin37 is the major connexin expressed in the media of caudal artery. Arterioscler Thromb Vasc Biol 22:1427–1432.

Rummery NM, Grayson TH, Hill CE. 2005. Angiotensin-converting enzyme inhibition restores endothelial but not medial connexin expression in hypertensive rats. J Hypertens 23:317–328.

Sato T, Haimovici R, Kao R, Li AF, Roy S. 2002. Downregulation of connexin 43 expression by high glucose reduces gap junction activity in microvascular endothelial cells. Diabetes 51:1565–1571.

Satoh M, Fujimoto S, Haruna Y, Arakawa S, Horike H, Komai N, Sasaki T, Tsujioka K, Makino H, Kashihara N. 2005. NAD(P)H oxidase and uncoupled nitric oxide synthase are major sources of glomerular superoxide in rats with experimental diabetic nephropathy. Am J Physiol 288:F1144–F1152.

Schalkwijk CG, Stehouwer CD. 2005. Vascular complications in diabetes mellitus: the role of endothelial dysfunction. Clin Sci (Lond) 109:143–159.

Segal SS. 2005. Regulation of blood flow in the microcirculation. Microcirculation 12:33–45.

Shiraishi M, Wang X, Walsh MP, Kargacin G, Loutzenhiser K, Loutzenhiser R. 2003. Myosin heavy chain expression in renal afferent and efferent arterioles: relationship to contractile kinetics and function. FASEB J 17:2284–2286.

Sladek SM, Westerhausen-Larson A, Roberts JM. 1999. Endogenous nitric oxide suppresses rat myometrial connexin 43 gap junction protein expression during pregnancy. Biol Reprod 61:8–13.

Szkudelski T. 2001. The mechanism of alloxan and streptozotocin action in B cells of the rat pancreas. Physiol Res 50:537–546.

Turoni CM, Reynoso HA, Maranon RO, Coviello A, Peral de Bruno M. 2005. Structural changes in the renal vasculature in streptozotocin-induced diabetic rats without hypertension. Nephron Physiol 99:50–57.

Yamashita T, Kawashima S, Ohashi Y, Ozaki M, Rikitake Y, Inoue N, Hirata K, Akita H, Yokoyama M. 2000. Mechanisms of reduced nitric oxide/cGMP-mediated vasorelaxation in transgenic mice overexpressing endothelial nitric oxide synthase. Hypertension 36:97–102.

Yao J, Hiramatsu N, Zhu Y, Morioka T, Takeda M, Oite T, Kitamura M. 2005. Nitric oxide-mediated regulation of connexin43 expression and gap junctional intercellular communication in mesangial cells. J Am Soc Nephrol 16:58–67.

Yuan BH, Robinette JB, Conger JD. 1990. Effect of angiotensin II and norepinephrine on isolated rat afferent and efferent arterioles. Am J Physiol 258:F741–F750.

Zaki FG, Keim GR, Takii Y, Inagami T. 1982. Hyperplasia of juxtaglomerular cells and renin localization in kidney of normotensive animals given captopril: electron microscopic and immunohistochemical studies. Ann Clin Lab Sci 12:200–215.

Zanetti M, Barazzoni R, Stebel M, Roder E, Biolo G, Baralle FE, Cattin L, Guarnieri G. 2005. Dysregulation of the endothelial nitric oxide synthase-soluble guanylate cyclase pathway is normalized by insulin in the aorta of diabetic rat. Atherosclerosis 181: 69–73.

Zhang J, Hill CE. 2005. Differential connexin expression in preglomerular and postglomerular vasculature: accentuation during diabetes. Kidney Int 68:1171–1185.

Research Paper

Journal of Vascular Research

J Vasc Res 2006;43:131–138
DOI: 10.1159/000090132

Received: March 28, 2005
Accepted after revision: September 23, 2005
Published online: December 7, 2005

Endothelial Urocortin Has Potent Antioxidative Properties and Is Upregulated by Inflammatory Cytokines and Pitavastatin

Tomoyuki Honjo[a] Nobutaka Inoue[a] Rio Shiraki[a] Seiichi Kobayashi[a]
Kazunori Otsui[a] Motonori Takahashi[a] Ken-ichi Hirata[a]
Seinosuke Kawashima[a] Hiroshi Yokozaki[b] Mitsuhiro Yokoyama[a]

[a]Division of Cardiovascular and Respiratory Medicine, Department of Internal Medicine, and [b]Division of Surgical Pathology, Department of Biological Informatics, Kobe University Graduate School of Medicine, Kobe, Japan

Key Words
Endothelium · Oxidative stress · HMG-CoA reductase inhibitors

Abstract
Background: Urocortin, a neuropeptide discovered in the midbrain, is a member of the corticotropin-releasing factor family and is expressed in heart tissues. Urocortin exerts potent cardioprotective effects under various pathological conditions including ischemia/reperfusion. However, the regulation and function of vascular urocortin are unknown. ***Methods and Results:*** Immunohistochemistry showed definitive expression of urocortin in endothelial cells of coronary large arteries and microvessels from autopsied hearts. RT-PCR confirmed the expression of urocortin in human umbilical vein endothelial cells (HUVECs). Urocortin (10^{-8} *M*) potently suppressed the generation of angiotensin II-induced reactive oxygen species (ROS) in HUVECs. Tumor necrosis factor-α and interferon-γ increased the urocortin mRNA levels and its release from HUVECs. Incubation with pitavastatin (0.1–3.0 μ*M*) significantly increased the urocortin mRNA levels and its release from HUVECs. Furthermore, treatment with pitavastatin (2 mg/day) for 4 weeks increased the serum urocortin level from 11.0 ± 6.5 to 16.4 ± 7.3 ng/ml in healthy volunteers. ***Conclusion:*** Endothelial urocortin was upregulated by inflammatory cytokines and pitavastatin and suppressed ROS production in endothelial cells. Treatment with pitavastatin increased the serum urocortin level in human subjects. Thus, endothelial urocortin might protect cardiomyocytes in inflammatory lesions. Urocortin might partly explain the mechanisms of various pleiotropic effects of statins.

Introduction

Urocortin is a 40-amino-acid peptide originally discovered in the rat midbrain and a member of the corticotropin-releasing factor (CRF) family [1]. Human urocortin is expressed not only in the central nervous system, such as in the pituitary [2] and brain [3], but also in various peripheral tissues, including the placenta [4], gastrointestinal tract [5], synovial tissue [6], lymphocytes [7], adipose tissue [8] and heart [9]. These findings suggest that urocortin has some pathophysiologic roles in these peripheral tissues. Especially in the heart, exogenous administration of urocortin induces cardiac inotropic ef-

KARGER
Fax +41 61 306 12 34
E-Mail karger@karger.ch
www.karger.com

1018–1172/06/0432–0131$23.50/0

Accessible online at:
www.karger.com/jvr

Dr. Nobutaka Inoue
Division of Cardiovascular and Respiratory Medicine, Department of Internal Medicine
Kobe University Graduate School of Medicine
7-5-2 Kusunoki-cho, Chuo-ku, Kobe 650-0017 (Japan)
Tel. +81 78 382 5846, Fax +81 78 382 5859, E-Mail nobutaka@ri.ncvc.go.jp

fects and coronary vasodilation [10–12]. Moreover, it was reported that exogenous urocortin has potent protective effects on myocardial cells during ischemia. For example, urocortin increases the survival of cultured cardiac cells exposed to ischemia and also rescues the infarct area of rat heart during ischemia/reperfusion [13–17].

The actions of the CRF family peptides are mediated by at least two types of G-protein-coupled receptors, CRF-R1 and CRF-R2 [1]. CRF-R2 exists in three alternative spliced forms, i.e., CRF-R2α, R2β, and R2γ. CRF-R2 is expressed in the cardiovascular system [18, 19], and has higher affinity for urocortin than CRF. Wiley et al. [19] reported that urocortin produced a potent and sustained vasodilator response in isolated human internal mammary artery. The coexpression of CRF-R2 with its preferred urocortin ligand in the heart suggests that urocortin-induced cardioprotective effects are likely mediated by CRF-R2 in an autocrine/paracrine manner [20]. Recently, Florio et al. [21] reported that urocortin is expressed in vessel walls. Furthermore, previous investigations demonstrated that CRF-R2 exists in cultured human umbilical vein endothelial cells (HUVECs) [22]. However, the vascular action of urocortin and its regulation remain unknown.

On the other hand, there is accumulating evidence that besides its potent lipid-lowering effect, HMG-CoA reductase inhibitors have pleiotropic effects such as anti-inflammatory [25, 26], anti-proliferative and anti-oxidative effects [27]. These drugs improve endothelial dysfunction in various pathologic conditions and stabilize vulnerable plaques via suppression of inflammation [28]. More recently, Node et al. [23] reported that HMG-CoA reductase inhibitors improve cardiac function in patients with heart failure. The potent cardioprotective effects suggest that the pleiotropic effects of HMG-CoA reductase inhibitors are related to urocortin.

In the present study, we investigated whether urocortin is expressed in human endothelial cells. We also investigated the vascular action of urocortin and what factors regulate the expression of endothelial urocortin. Furthermore, the interaction of urocortin and HMG-CoA reductase inhibitor was investigated.

Methods

Cell Culture

HUVECs were obtained from Sanko Junyaku (Japan) and cultured in Medium 199 with 20% fetal bovine serum (FBS), 100 IU/ml heparin (Sigma Chemical Co., St. Louis, Mo., USA), 100 IU/ml endothelial cell growth supplement (BD Biosciences, Franklin Lakes, N.J., USA), 100 U/ml penicillin, and 100 μg/ml streptomycin. Cells were used between passages 4 and 8. Cells were stimulated with tumor necrosis factor-α (TNF-α), interferon-γ (IFN-γ), or pitavastatin at various concentrations for the indicated hours (0, 3, 6, and 24 h) in the presence of 5% FBS. Human recombinant TNF-α and IFN-γ were purchased from R&D Systems, Inc. (Mckinley Place NE, Minn., USA) and Diaclone Research (France), respectively. Pitavastatin was obtained from Kowa Pharmaceutical Company (Tokyo, Japan). After stimulation, the culture medium was collected for enzyme-linked immunosorbent assay (ELISA), and the cells were used for RNA isolation.

Measurement of Urocortin by ELISA

Serum urocortin and supernatants of cell culture medium were assayed by ELISA (Phoenix Pharmaceuticals Inc., Belmont, Calif., USA) according to the manufacturer's instructions. Assays were performed in polystyrene 96-well plates. The urocortin concentration was quantified against a standard curve calibrated with known amounts of protein. The upper detection limit for urocortin was 100 ng/ml. Each value is the mean of duplicate measurements.

Human Blood Sample and Study Design

Fifteen male volunteers, 25–41 years old, were included in the study. Participants were examined to exclude any pathologic disorders, which was confirmed with blood tests. Three volunteers were excluded because of mildly elevated levels of creatine phosphokinase or C-reactive protein (CRP). The remaining healthy subjects were treated with pitavastatin (2 mg/day) for 4 weeks. Blood samples were collected before and after pitavastatin treatment, and serum levels of lipids, CRP, and urocortin were measured. There were no reported adverse effects of pitavastatin. Written informed consent was obtained from all participants.

Immunohistochemistry

Immunohistochemistry for urocortin was performed on serial cryostat sections cut at 6 μm from frozen human coronary artery and heart muscle specimens. The sections were blocked with carrier protein for 30 min at room temperature, and then incubated with a primary antibody (rabbit anti-urocortin, IgG fraction of antiserum, Sigma Chemical Co.) (diluted 1:200) overnight at 4°C. The final concentration of primary antibody was 40 μg/ml. The sections were washed with phosphate-buffered saline (PBS), incubated with biotinylated goat anti-rabbit immunoglobulins (Dako) (diluted 1:500), washed in PBS, and finally incubated with streptavidin horseradish peroxidase conjugate (Dako LSAB kit™, Dako). For negative controls, the primary antibody was replaced with rabbit nonspecific immunoglobulin.

Reverse Transcription PCR and Measurement of Urocortin RNA Level

Total RNA was isolated from cultured HUVECs using a total RNA isolation kit (Isogen; Nippon Gene, Japan) according to the manufacturer's instructions. Complementary DNA was prepared using an RT-PCR kit (RETROscript™; Ambion). PCR were performed with *Taq* polymerase using the following specific primers. The primer sequences were as follows: human urocortin sense primer 5′-CAGGCGAGCGGCCGCG-3′, human urocortin antisense primer 5′-CTTGCCCACCGAGTCGAAT-3′. Urocortin cDNA amplification was performed in 40 cycles: samples were heated to 94°C for 1 min, cooled to 60°C for 1 min, and then heat-

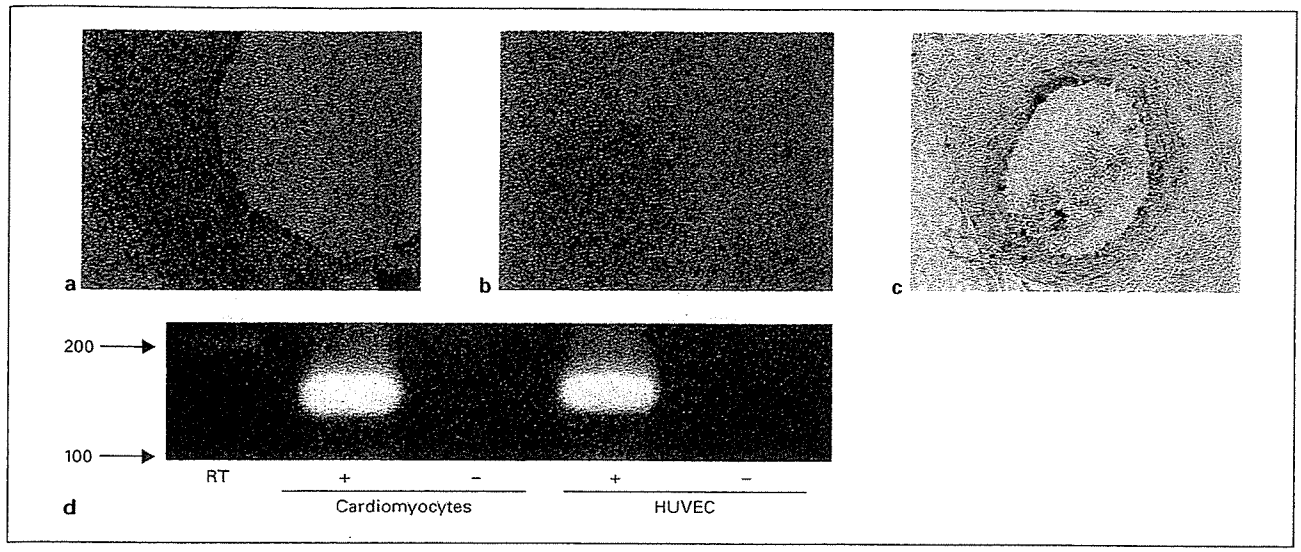

Fig. 1. Expression of urocortin in human endothelial cells. **a**, **c** Immunohistochemical analysis using epicardial coronary arteries (**a**) and microvessels in heart muscle (**c**) obtained from autopsy cases demonstrated positive urocortin immunoreactivity. **b** There was no significant staining when nonimmune serum was used as a control. **d** RT-PCR confirmed the expression of urocortin in cultured HUVECs. Human cardiomyocytes were used as a positive control.

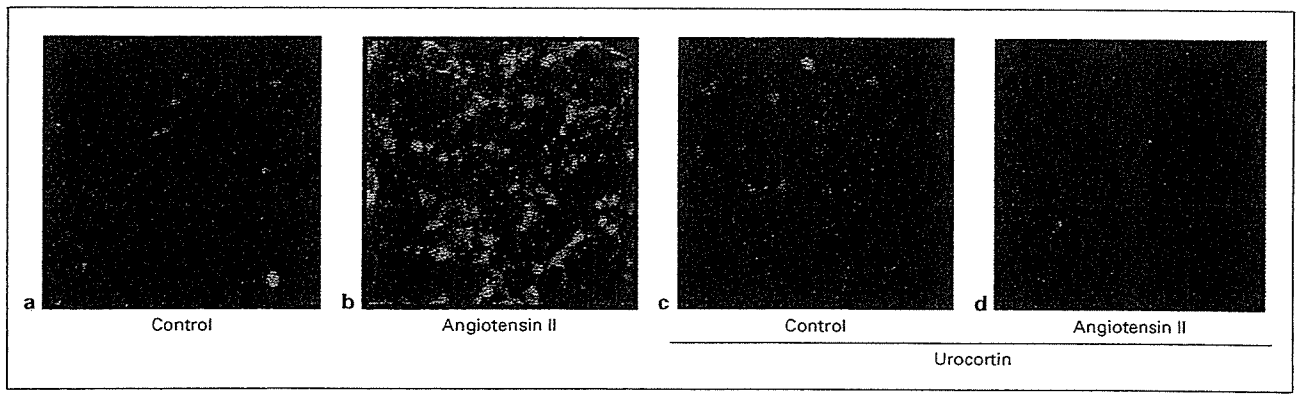

Fig. 2. Effects of urocortin on intracellular ROS in HUVECs assessed by the H_2DCFDA method. **a**, **b** Incubation with angiotensin II (10^{-7} *M*) induced the generation of intracellular ROS in HUVECs. **c**, **d** Coincubation with urocortin (10^{-8} *M*) significantly suppressed angiotensin II-induced intracellular ROS generation.

ed at 72°C for 1 min. PCR products were separated using 2% agarose gels stained with ethidium bromide and visualized under UV light. PCR products were purified and further analyzed by DNA sequencing using an ABI Prism BigDye Terminator Cycle Sequencing kit on an ABI Prism 310 Genetic Analyzer. To measure the production of urocortin mRNA, RT-PCR for GAPDH was also performed (sense primer 5′-ACGGATTTGGTCGTATTGGGC-3′, antisense primer 5′-TTGACGGTGCCATGGAATTTG-3′). Photographs of the ethidium-bromide-stained gels were scanned, and band intensities were measured using a densitometer (ATTO Lane Analyzer 3.0; ATTO Co., Tokyo, Japan). The quantity of the urocortin mRNA was determined by the ratio of urocortin and GAPDH band intensities.

Evaluation of Intracellular ROS in HUVECs

Intracellular ROS were detected with 2′,7-dichlorodihydrofluoresceindiacetate (H_2DCFDA, Molecular Probes, Eugene, Oreg., USA). As described before [31], a confluent monolayer of HUVECs was treated with angiotensin II (10^{-7} *M*) (Sigma Chemical Co.) or human urocortin (10^{-8} *M*) (Phoenix Pharmaceuticals Inc.) for 1 h,

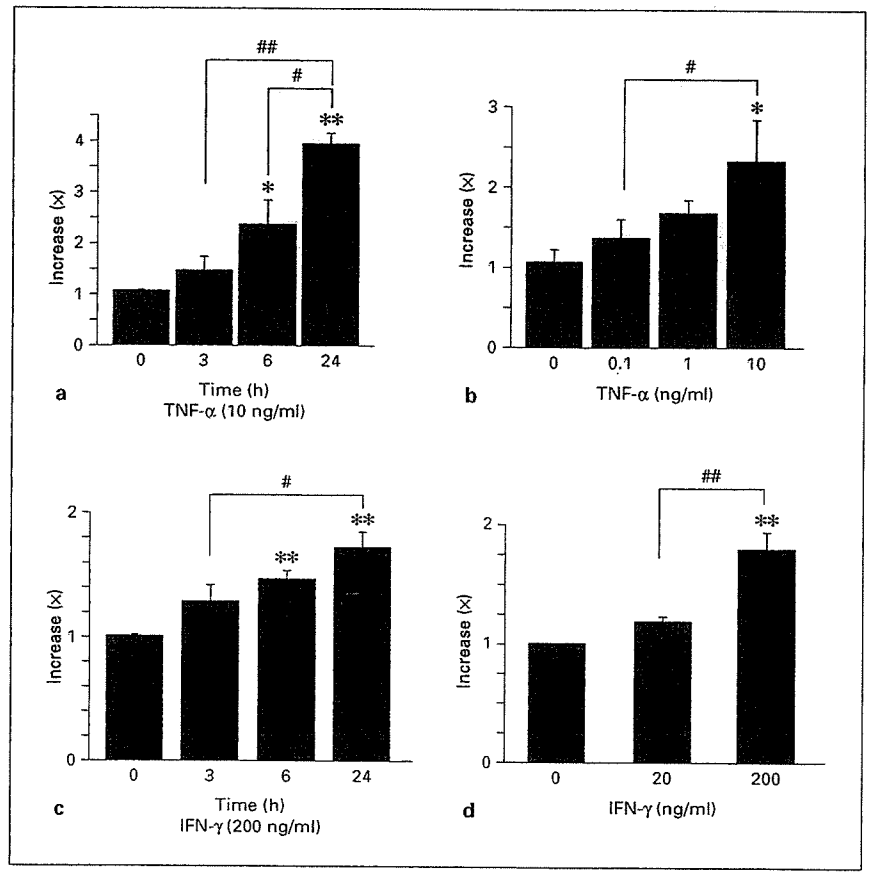

Fig. 3. Effects of TNF-α (**a**, **b**) or IFN-γ (**c**, **d**) on the release of urocortin from HUVECs. **a**, **b** HUVECs were incubated with TNF-α (10 ng/ml) for the indicated time periods (**a**) or for 6 h with the indicated concentration of TNF-α (**b**). **c**, **d** HUVECs were incubated with IFN-γ (200 ng/ml) for the indicated time periods (**c**) or for 6 h with the indicated concentration of IFN-γ (**d**). After stimulation, the concentration of urocortin in the conditioned medium was assessed by ELISA. Data were plotted as mean ± SEM from three independent experiments performed in duplicate. * $p < 0.05$; ** $p < 0.01$ vs. control; # $p < 0.05$; ## $p < 0.01$.

then they were treated with H_2DCFDA (10 μ*M*) for 30 min at 37°C in the dark. The fluorescence intensity was measured using a laser-scanning confocal imaging system.

Statistical Analysis

Data are presented as mean ± SEM. Statistical analysis was performed by analysis of variance followed by Fisher's PLSD test. $p < 0.05$ was considered to be statistically significant.

Results

Human Endothelial Cells Express Urocortin

First, we examined whether human endothelial cells express urocortin. As shown in figure 1, immunohistochemical analysis using specimens obtained from autopsy cases demonstrated positive immunoreactivity of urocortin in human epicardial coronary artery endothelial cells (fig. 1a) and endothelial cells of microvessels in heart muscle (fig. 1c), whereas there was no signal when non-immune serum was used (fig. 1b). Preabsorbance of the primary antibody with 10^{-8}–10^{-6} *M* of urocortin significantly suppressed the immunoreactivity. Next, to confirm its expression in endothelial cells, RT-PCR was performed using sets of urocortin-specific primers. Urocortin mRNA was detected by RT-PCR in HUVECs (fig. 1d). No RT-PCR product was present in the negative control in which RT was not performed. Sequencing of complementary DNA of urocortin obtained from HUVECs was the same as the sequence obtained from neurons (data not shown). Thus, urocortin is expressed in human endothelial cells.

Urocortin Suppressed ROS Generation in HUVECs

We investigated the effects of urocortin on ROS generation of HUVECs by H_2DCFDA. Incubation with angiotensin II (10^{-7} *M*) induced the generation of ROS in HUVECs (fig. 2). Urocortin (10^{-8} *M*) significantly suppressed angiotensin II-induced ROS generation.

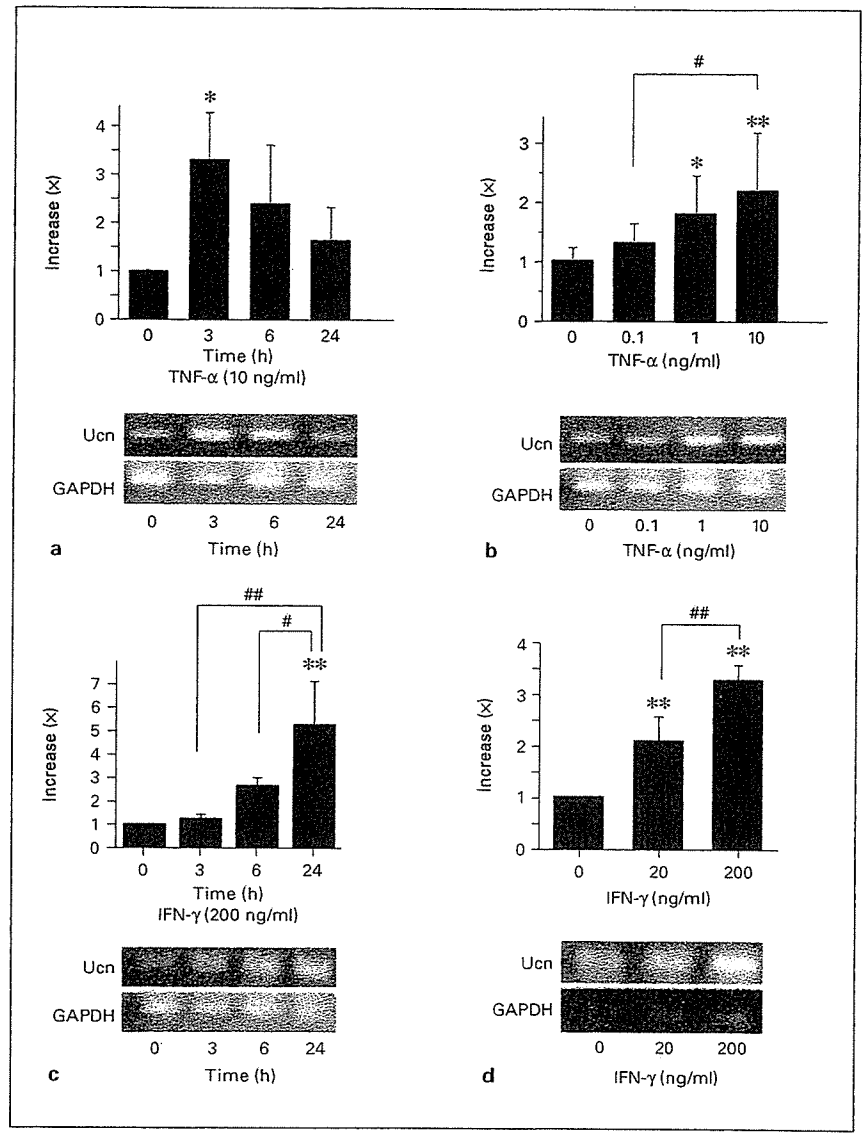

Fig. 4. Effects of TNF-α (**a**, **b**) or IFN-γ (**c**, **d**) on urocortin (Ucn) mRNA in HUVECs assessed by RT-PCR. **a**, **b** HUVECs were incubated with TNF-α (10 ng/ml) for the indicated time periods (**a**) or for 6 h with the indicated concentration of TNF-α (**b**). **c**, **d** HUVECs were incubated with IFN-γ (200 ng/ml) for the indicated time periods (**c**) or for 6 h with the indicated concentration of IFN-γ (**d**). After stimulation, mRNA levels of urocortin were assessed by RT-PCR. Densitometric analysis of five independent experiments. * $p<0.05$; ** $p<0.01$ vs. control; # $p<0.05$; ## $p<0.01$.

Expression of Endothelial Urocortin Was Increased by Inflammatory Cytokines and Pitavastatin

Because previous studies demonstrated that various cytokines modulate the expression of urocortin in neurons, the effects of inflammatory cytokines on expression of endothelial urocortin were examined by ELISA. Incubation with TNF-α (10 ng/ml) resulted in increased urocortin production in a time- and dose-dependent manner (fig. 3a, b). IFN-γ also increased the urocortin release from HUVECs (fig. 3c, d).

RT-PCR demonstrated that TNF-α and IFN-γ increased the steady state urocortin mRNA levels in HUVECs (fig. 4). Incubation with pitavastatin (0.1–3.0 μ*M*) potently increased the release of urocortin from HUVECs in a dose-dependent manner (fig. 5a). RT-PCR revealed modestly increased urocortin mRNA from HUVECs (fig. 5b).

Treatment with Pitavastatin Increases Serum Urocortin Levels in Humans

The findings using cultured HUVECs prompted us to examine the effects of treatment with pitavastatin on plasma urocortin levels in humans. Treatment with pitavastatin (2 mg/day) for 4 weeks decreased total cho-

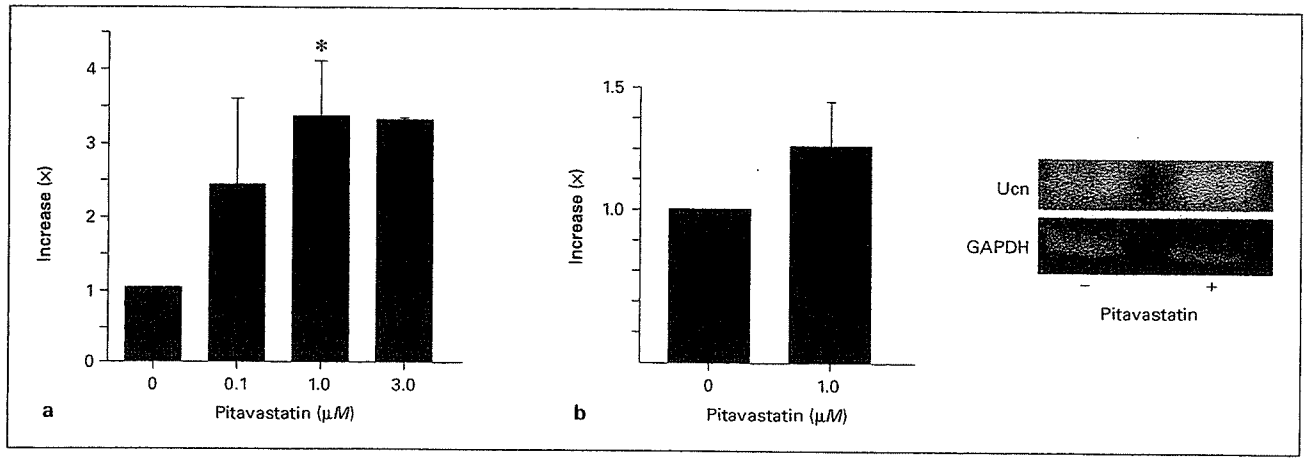

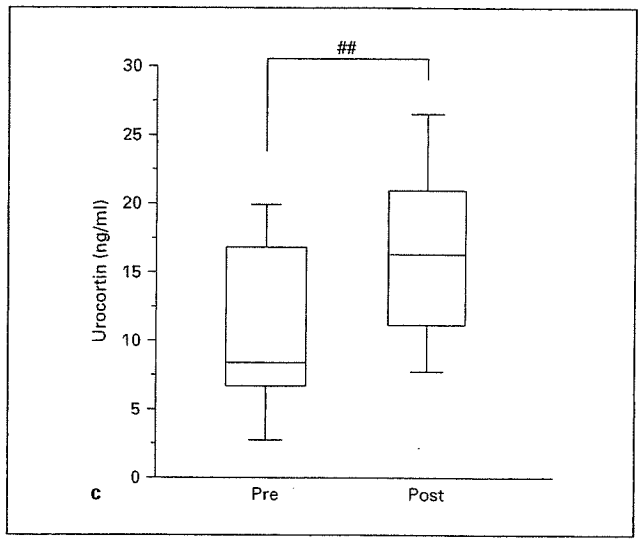

Fig. 5. a, b Effects of pitavastatin on urocortin release (**a**) and its mRNA (**b**) in HUVECs. HUVECs were incubated with pitavastatin with the indicated concentration for 24 h. After stimulation, the concentration of urocortin in the conditioned medium was assessed by ELISA (**a**). Data were plotted as mean ± SEM from three independent experiments, performed in duplicate. Pitavastatin-induced changes in urocortin mRNA were assessed by RT-PCR (**b**). Densitometric analysis of three independent experiments. * $p < 0.05$ vs. control. **c** Treatment with pitavastatin increases serum levels of urocortin in humans. Treatment with pitavastatin (2 mg/day) for 4 weeks increased urocortin levels in healthy male volunteers. ## $p < 0.01$.

Table 1. Change of serum levels of various parameters by pitavastatin

Charasteristics	Mean ± SD (pre)	Mean ± SD (post)
Blood glucose	96 ± 10.4	93 ± 6.5
Total cholesterol, mg/dl	192.8 ± 29.7	149.2 ± 27.4***
TG, mg/dl	88.4 ± 44.6	86.4 ± 40.3
HDL cholesterol, mg/dl	69.6 ± 15.1	67 ± 15.3
LDL cholesterol, mg/dl	100.0 ± 25.4	61.0 ± 22.5***
hsCRP, ng/ml	257.5 ± 235.9	254.1 ± 248.6
Serum urocortin, ng/ml	11.0 ± 6.5	16.4 ± 7.3**

Treatment with pitavastatin (2 mg/day) for 4 weeks significantly decreased total cholesterol and LDL cholesterol levels. Pitavastatin significantly increased serum urocortin levels. *** $p < 0.0001$ vs. pre. ** $p < 0.01$ vs. pre.

lesterol and LDL levels (table 1). Interestingly, pitavastatin increased urocortin levels from 11.0 ± 6.5 to 16.4 ± 7.3 ng/ml in healthy male volunteers (fig. 5c).

Discussion

Urocortin was originally identified in the central nervous system [1–3]; however, there is considerable evidence indicating that urocortin is also expressed in other organs, including the gastrointestinal [5], immune [6, 7] and cardiovascular systems [9]. There is no direct evidence, however, that urocortin is expressed in the vasculature. The present investigation is the first study to demonstrate that urocortin is expressed in endothelial cells.

Furthermore, urocortin (10^{-8} *M*) potently suppressed ROS generation induced by angiotensin II in HUVECs. TNF-α and IFN-γ increased urocortin mRNA level and its release from HUVECs. Interestingly, incubation with pitavastatin significantly increased urocortin mRNA levels and its release from HUVECs. Thus, endothelial urocortin is upregulated by inflammatory cytokines and pitavastatin, and it has anti-oxidative properties in endothelial cells. Furthermore, treatment with pitavastatin for 4 weeks increased the serum urocortin levels in healthy male volunteers.

Urocortin is expressed in various immunocompetent cells such as macrophages and lymphocytes [7], and in inflammatory lesions. For example, Kohno et al. [6] reported that urocortin is expressed in the synovium of rheumatoid arthritis patients. The expression of immunoreactive urocortin in rheumatoid arthritis patients correlates with the extent of inflammatory infiltrates [6]. On the other hand, the concentration of immunoreactive urocortin was higher in gastric biopsies obtained from patients with active *Helicobacter pylori* gastritis than in normal controls [5]. After the apparent eradication of *H. pylori* infection, immunoreactive urocortin levels increased dramatically compared with pretreatment values. These findings strongly suggest that urocortin has a possible role in the pathogenesis of these inflammatory diseases. There remains controversy, however, as to whether urocortin exerts proinflammatory or anti-inflammatory effects. Urocortin increases the secretion of interleukin-6 from peripheral blood mononuclear cells [6], suggesting it has proinflammatory actions. In contrast, Agnello et al. [24] reported that urocortin significantly reduces lipopolysaccharide-induced serum TNF-α and interleukin-1β levels in mice. In the present investigation, urocortin potently suppressed ROS generation in HUVECs, whereas inflammatory cytokines increased urocortin expression and its release from HUVECs. Taken together, these findings suggest that endothelial urocortin acts as an anti-oxidative factor, and the upregulation of urocortin by inflammatory cytokines is part of a counter-regulatory mechanism against oxidative stress in inflammatory lesions.

Recently, a wide variety of pleiotropic effects of HMG-CoA reductase inhibitors was proposed, including improvement of endothelial function, stabilization of vulnerable plaque, anti-coagulation effects, anti-inflammatory effects, anti-oxidative effects, etc. [29, 30]. Treatment with HMG-CoA reductase inhibitors improves the functional classification of the New York Heart Association and left ventricular ejection fraction in patients with dilated cardiomyopathy [23]. Furthermore, plasma concentrations of TNF-α, interleukin-6, and brain natriuretic peptide are also significantly decreased by HMG-CoA reductase inhibitor treatment [23]. Thus, HMG-CoA reductase inhibitors likely induce potent cardioprotective effects. In the present study, pitavastatin increased the release of urocortin from HUVECs. There was no statistically significant increase in urocortin mRNA levels after incubation with pitavastatin, although mRNA levels tended to increase. Posttranscriptional regulation may mediate the increase in urocortin mRNA levels during incubation with pitavastatin. Furthermore, treatment with pitavastatin increased the serum urocortin levels in humans. Given its potent cardioprotective effects, urocortin might be partly involved in the mechanisms of the pleiotropic effects of HMG-CoA reductase inhibitors in the vasculature. The pitavastatin-induced increase in urocortin may originate from several possible sources, including the central and peripheral nervous systems, cardiomyocytes, and endothelial cells. Further investigation is needed to clarify the precise mechanisms whereby pitavastatin increases the serum urocortin levels.

In conclusion, urocortin was expressed in human endothelial cells. Endothelial urocotin is upregulated by inflammatory cytokines and pitavastatin, and it suppressed the production of ROS in endothelial cells. Treatment with pitavastatin increased the serum urocortin levels in human subjects. Endothelial urocortin might exert anti-oxidative effects in inflammatory lesions and this might partially explain the mechanisms of various pleiotropic effects of statins.

References

1 Vaughan J, Donaldson C, Bittencourt J, Perrin MH, Lewis K, Sutton S, Chan R, Turnbull AV, Lovejoy D, River C: Urocortin, a mammalian neuropeptide related to fish urotensin 1 and to corticotrophin-releasing factor. Nature 1995; 378:287–292.

2 Iino K, Sasano H, Oki Y, Andoh N, Shin RW, Kitamoto T, Totsune K, Suzuki H, Nagura H, Yoshimi T: Urocortin expression in human pituitary gland and pituitary adenoma. J Clin Endocrinol Metab 1997;82:3842–3850.

3 Takahashi K, Totsune K, Sone M, Murakami O, Satoh F, Arihara Z, Sasano H, Iino K, Mouri T: Regional distribution of urocortin-like immunoreactivity and expression of urocortin mRNA in the human brain. Peptide 1998;19: 643–647.

4 Petraglia F, Florio P, Gallo R, Simoncini T, Saviozzi M, Di Blasio AM, Vaughan J, Vale W: Human placenta and fetal membranes express human urocortin mRNA and peptide. J Clin Endocrinol Metab 1996;81:3807–3810.

5 Chatzaki E, Charalampopolos I, Leontidis C, Mouzas IA, Tzardi M, Tsatsanis C, Margioris AN, Gravanis A: Urocortin in human gastric mucosa: relationship to inflammatory activity. J Clin Endocrinol Metab 2003;88:478–483.

6 Kohno M, Kawahito Y, Tsubouchi Y, Hashiramoto A, Yamada R, Inoue K, Kusaka Y, Kubo T, Elenkov IJ, Chrousos G, Kondo M, Sano H: Urocortin expression in synovium of patients with rheumatoid arthritis and osteoarthritis: relation to inflammatory activity. J Clin Endocrinol Metab 2001;86:4344–4352.

7 Bamberger CM, Wald M, Bamberger AM, Ergun S, Beri FU, Schulte HM: Human lymphocytes produce urocortin, but not corticotropin-releasing hormone. J Clin Endocrinol Metab 1998;83:708–711.

8 Seres J, Bornstein SR, Seres P, Willenberg HS, Schulte KM, Scherbaum WA, Ehrhart-Bornstein M: Corticotropin-releasing hormone system in human adipose tissue. J Clin Endocrinol Metab 2004;89:965–970.

9 Kimura Y, Takahashi K, Totsune K, Muramatsu Y, Kaneko C, Darnel AD, Suzuki T, Ebina M, Nukiwa T, Sasano H: Expression of urocortin and corticotrophin-releasing factor receptor subtypes in the human heart. J Clin Endocrinol Metab 2002;87:340–346.

10 Rademaker MT, Charles CJ, Espiner E, Fisher S, Frampton CM, Kirkpatrick CMJ, Lainchbury J, Nicholls G, Richards M, Vale W: Beneficial hemodynamic, endocrine, and renal effects of urocortin in experimental heart failure: comparison with normal sheep. J Am Coll Cardiol 2002;40:1495–1505.

11 Huag Y, Chan F, Lau CW, Tsang SY, Chen ZY, He GW, Yao X: Roles of cyclic AMP and Ca^{2+}-activated K^+ channels in endothelium-independent relaxation by urocortin in the rat coronary artery. Cardiovascular Research 2003;57:824–833.

12 Parkes DG, Vaughan J, Rivier J, Vale W, May CN: Cardiac inotropic actions of urocortin in conscious sheep. Am J Physiol 1997;272: H2115–H2122.

13 Scarabelli TM, Pasini E, Stephanou A, Comini L, Curello S, Raddino R, Ferrari R, Knight R, Latchman D: Urocortin promotes hemodynamic and bioenergic recovery and improves cell survival in the isolated rat heart exposed to ischemia/reperfusion. J Am Coll Cardiol 2002;40:155–161.

14 Gordon JM, Gregory JD, Owen LW, Dusting GJ, Woodman OL: Cardioprotective action of CRF peptide urocortin against stimulated ischemia in adult rat cardiomyocytes. Am J Physiol Heart Circ Physiol 2003;284:H330–H336.

15 Lawrence KM, Chanalaris A, Scarabelli T, Hubank M, Pasini E, Townsend PA, Comini L, Ferrari R, Tinker A, Stephanou A, Kight R, Litchman D: K_{ATP} channel gene expression is induced by urocortin and mediates its cardioprotective effect. Circulation 2002;106:1556–1562.

16 Schulman D, Latchman DS, Yellon DM: Urocortin protects the heart from reperfusion injury via upregulation of p42/p44 MAPK signaling pathway. Am J Physiol Heart Circ Physiol 2002;283:H1481–H1488.

17 Brar BK, Jonassen AK, Stephanou A, Santilli G, Railson J, Knight RA, Yellon DM, Latchman DS: Urocortin protects against ischemic and reperfusion injury via a MAPK-dependent pathway. J Biol Chem 2000;275:8508–8514.

18 Kishimoto T, Pearse RV, Lin CR, Rosenfeld MG: A sauvagine/corticotrophin-releasing factor receptor expressed in heart and skeletal muscle. Proc Natl Acad Sci USA 1995;92: 1108–1112.

19 Wiley KE, Davenport AP: CRF2 receptors are highly expressed in the human cardiovascular system and their cognate ligands urocortins 2 and 3 are potent vasodilators. Br J Pharmacol 2004;143:508–514.

20 Coste SC, Kesterson RA, Heldwein KA, Stevens SL, Heard AD, Hollis JH, Murray SE, Hill JK, Pantely GA, Hohimer AR, Hatton DC, Phillips TJ, Finn DA, Low MJ, Rittenberg MB, Stenzel P, Stenzel-Poore MP: Abnormal adaptations to stress and impaired cardiovascular function in mice lacking corticotropin-releasing hormone receptor-2. Nat Genet 2000;24: 403–409.

21 Florio P, Arcuri F, Ciarmela P, Runci Y, Romagnoli R, Cintorino M, Di Blasio AM, Petraglia F: Identification of urocortin mRNA and peptide in the human endometrium. J Endocrinol 2002;173:R9–R14.

22 Simoncini T, Apa R, Reis FM, Miceli F, Stomati M, Driul L, Lanzone A, Genazzani AR, Petraglia F: Human umbilical vein endothelial cells: a new source and potential target for corticotropin-releasing factor. J Clin Endocrinol Metab 1999;84:2802–2806.

23 Node K, Fujita M, Kitakaze M, Hori M, Liao JK: Short-term statin therapy improves cardiac function and symptom in patients with idiopathic dilated cardiomyopathy. Circulation 2003;108:839–843.

24 Agnello D, Bertini R, Sacco S, Meazza C, Villa P, Ghezzi P: Corticosteroid-independent inhibition of tumor necrosis factor production by the neuropeptide urocortin. Am J Physiol 1998;275:E757–E762.

25 Ridker PM, Rifai N, Pfeffer MA, Sacks F, Braunwald E: Long-term effects of pravastatin on plasma concentration of C-reactive protein. Circulation 1999;100:230–235.

26 Ridker PM, Rifai N, Lowenthal SP: Rapid reduction in C-reactive protein with cerivastatin among 785 patients with primary hypercholesterolemia. Circulation 2001;103:1191–1193.

27 Rikitake Y, Kawashima S, Takeshita S, Yamashita T, Azumi H, Yasuhara M, Nishi H, Inoue N, Yokoyama M: Anti-oxidative properties of fluvastatin, an HMG-CoA reductase inhibitor, contribute to prevention of atherosclerosis in cholesterol-fed rabbits. Atherosclerosis 2001;154:87–96.

28 Treasure CB, Klein L, Weintraub WS, Talley JD, Stillabower ME, Kosinski AS, Zhang J, Boccuzzi S, Cedarholm J, Alexander W: Beneficial effects of cholesterol-lowering therapy on the coronary endothelium in patients with coronary artery disease. N Engl J Med 1995; 332:481–487.

29 Takamoto M, Liao JK: Pleiotropic effects of 3-hydoxy-3-methylglutaryl coenzyme A reductase inhibitors. Arterioscler Tromb Vasc Biol 2001;21:1712–1719.

30 Liao JK: Beyond lipid lowering: the role of statins in vascular protection. Int J Cardiol 2002;86:5–18.

31 Kobayashi S, Inoue N, Ohashi Y, Terashima M, Matsui K, Mori T, Fujita H, Awano K, Kobayashi K, Azumi H, Ejiri J, Hirata K, Kawashima S, Hayashi Y, Yokozaki H, Itoh H, Yokoyama M: Interaction of oxidative stress and inflammatory response in coronary plaque instability: important role of C-reactive protein. Arterioscler Thromb Vasc Biol 2003;23: 1398–1404.

Experimental Physiology

Cardiovascular Control: Relationships between nitric oxide-mediated endothelial function, eNOS coupling and blood pressure revealed by eNOS–GTP cyclohydrolase 1 double transgenic mice

D. Adlam, J. K. Bendall, J. P. De Bono, N. J. Alp, J. Khoo, T. Nicoli, M. Yokoyama, S. Kawashima and K. M. Channon

Exp Physiol 2007;92;119-126; originally published online Sep 28, 2006;

DOI: 10.1113/expphysiol.2006.035113

Experimental Physiology

Relationships between nitric oxide-mediated endothelial function, eNOS coupling and blood pressure revealed by eNOS–GTP cyclohydrolase 1 double transgenic mice

D. Adlam[1], J. K. Bendall[1], J. P. De Bono[1], N. J. Alp[1], J. Khoo[1], T. Nicoli[1], M. Yokoyama[2], S. Kawashima[2] and K. M. Channon[1]

[1]*Department of Cardiovascular Medicine, University of Oxford, Wellcome Trust Centre for Human Genetics, Roosevelt Drive, Oxford OX3 9DU, UK*
[2]*Kobe University of Medicine, Japan*

Endothelium-dependent relaxation in conduit vessels is mediated largely by nitric oxide (NO), produced by the enzyme endothelial nitric oxide synthase (eNOS) in the presence of the cofactor tetrahydrobiopterin (BH4) and mediated through a cGMP-dependent downstream signalling cascade. Endothelial NOS regulates blood pressure *in vivo*, and impaired endothelial NO bioactivity in vascular disease states may contribute to systemic hypertension. In the absence of sufficient levels of the cofactor BH4, NO becomes uncoupled from arginine oxidation and eNOS produces superoxide rather than NO. The enzymatic uncoupling of eNOS is an important feature of vascular disease states associated with increased oxidative stress. However, whether eNOS coupling, rather than overall eNOS activity, has specific effects on endothelium-dependent vasorelaxation *in vitro*, or on blood pressure regulation *in vivo*, remains unclear. In this study, we evaluate the relationships between blood pressure and endothelial function in models of eNOS uncoupling, using mice with endothelium-targeted transgenic eNOS overexpression (eNOS-Tg), in comparison with littermates in which eNOS coupling was rescued by additional endothelium-targeted overexpression of GTP cyclohydrolase 1 (eNOS/GCH-Tg) to increase endothelial BH4 levels. Despite the previously characterized differences in eNOS-dependent superoxide production between these animals, we find that blood pressure is equally reduced in both genotypes, compared with wild-type animals. Furthermore, both eNOS-Tg and eNOS/GCH-Tg mice exhibit similarly impaired endothelium-dependent vasorelaxation. We show that reduced vasorelaxation responses result from desensitization of cGMP-mediated signalling and are associated with increased NO production rather than changes in superoxide production.

(Received 17 July 2006; accepted after revision 18 September 2006; first published online 28 September 2006)
Corresponding author K. M. Channon: Department of Cardiovascular Medicine, University of Oxford, John Radcliffe Hospital, Oxford, OX3 8DU, UK. Email: keith.channon@cardiov.ox.ac.uk

The endothelium plays a central role in regulating vascular smooth muscle tone and blood pressure through the production of nitric oxide (NO) by the homodimeric enzyme endothelial nitric oxide synthase (eNOS; Furchgott & Zawadzki, 1980; Ignarro, 2002). Nitric oxide levels are a function of NO synthesis by eNOS and NO scavenging by reactive oxygen species (ROS). Reduced NO bioavailability is an important feature of vascular disease states, including hypertension, diabetes and atherosclerosis, in both humans and animal models (Kiff *et al.* 1991; Panza *et al.* 1995; Heitzer *et al.* 2001; Laursen *et al.* 2001; Alp *et al.* 2003; Henry *et al.* 2004). The importance of eNOS-derived NO for blood pressure regulation is supported by evidence of systemic hypertension in the eNOS knockout mouse (Huang *et al.* 1995; Shesely *et al.* 1996; Kojda *et al.* 1999) and hypotension in eNOS transgenic (eNOS-Tg) animals (Ohashi *et al.* 1998; van Haperen *et al.* 2002).

While these observations establish the basis for a relationship between eNOS protein levels, NO-mediated

D. Adlam, J. K. Bendall and J P. De Bono contributed equally to this work.

DOI: 10.1113/expphysiol.2006.035113

endothelial function and blood pressure, recent evidence suggests that physiological regulation of eNOS is more complex. The pteridine cofactor tetrahydrobiopterin (BH4) is critical for eNOS enzymatic activity, hence NO production. In the absence of adequate levels of BH4, eNOS becomes 'uncoupled' from L-arginine oxidation and instead molecular oxygen is reduced to form superoxide (Vasquez-Vivar *et al.* 1998, 2003; Landmesser *et al.* 2003). Although transgenic mice with endothelium-targeted eNOS overexpression have increased NO production and low blood pressure (Ohashi *et al.* 1998; van Haperen *et al.* 2002), the greatly increased levels of eNOS in these animals leads to eNOS uncoupling that is related to eNOS–BH4 stoichiometry in the endothelium (Bendall *et al.* 2005). Specifically, transgenic mice with endothelial eNOS overexpression have a marked increase in eNOS-derived superoxide production, owing to eNOS uncoupling, that is normalized by augmentiion of the endothelial BH4 levels by crossing with transgenic mice with endothelial expression of GTP cyclohydrolase 1 (GCH), the rate limiting enzyme in BH4 biosythesis (Bendall & Channon, 2005). However, it is not known whether the effects of coupled *versus* uncoupled eNOS on local NO and superoxide production have important effects on haemodynamic regulation. In particular, it remains unclear whether NO production alone, or other functionally related radicals such as superoxide, is the key determinant of vasorelaxation responses in isolated vessels, and how the changes in vasorelaxation remain quantitatively related to changes in blood pressure *in vivo*.

In this paper, we compare changes in blood pressure, NOS activity and vascular relaxation responses in endothelium-targeted transgenic mice with overexpression of either eNOS or GTP cyclohydrolase I, and in double transgenic mice with both eNOS and GCH overexpression. We demonstrate that blood pressure is determined principally by NO production rather than eNOS coupling, and that chronic increases in vascular NO production lead to desensitization of downstream cGMP-mediated signalling, independent of eNOS uncoupling.

Methods

Animals

Studies were performed in accordance with the UK Home Office Animals (Scientific Procedures) Act 1986. Mice were provided with standard chow and water *ad libitum* and housed singly at 24°C in individually ventilated cages (Techniplast Inc., Buguggiate, Italy). All mice were exposed to a regular 12 h–12 h light–dark cycle and were 11–18 weeks old at the time of study.

Mouse lines had previously been fully back-crossed onto C57bL/6 strain. Endothelial nitric oxide synthase transgenic mice (eNOS-Tg) were generated by targeting bovine eNOS overexpression to vascular endothelium under the control of the murine preproendothelin-1 promoter, as previously described (Ohashi *et al.* 1998). These animals have been shown to have an eightfold elevation in eNOS protein levels in lung and aortic tissue, with transgene expression confined to the endothelium (Ohashi *et al.* 1998; Bendall & Channon, 2005). Guanosine tripohosphate cyclohydrolase 1 transgenic mice (GCH-Tg) were generated by endothelium-targeted overexpression of human GCH under the control of the murine Tie-2 promoter, as previously described (Alp *et al.* 2003, 2004). These animals have been shown to have a threefold increase in tissue BH4 levels in lung, heart and aortic tissue (Alp *et al.* 2003; Bendall & Channon, 2005). eNOS-Tg and GCH-Tg heterozygote mice were crossbred to produce eNOS/GCH double Tg, eNOS-Tg, GCH-Tg and wild-type (WT) littermates in a 1:1:1:1 ratio for study. All animals were genotyped by polymerase chain reactions (PCR) on DNA prepared by phenol–chloroform extraction of ear-notch biopsies. Genotypes were double-checked using DNA prepared from lung tissue snap frozen at the time of killing.

Haemodynamic studies

Blood pressure was measured by direct invasive methods under general anaesthesia using the Millar® catheter system. Animals were anaesthetized using inhalational isofluorane vaporised on oxygen and maintained at a temperature of 36.5°C using a warming blanket. Surgical anaesthesia was determined by loss of the pedal withdrawal reflex. A mid-line incision was made in the neck, and the left carotid artery isolated. The cranial end of the artery was tied using 3.0 mersilk, and a stay suture looped around the caudal artery. A 1.5 F Millar® catheter was then introduced and advanced until a good blood pressure waveform trace could be detected. The proximal suture was then tied to provide haemostasis. Experimental anaesthesia was lightened to obtain a respiratory rate of 80 min^{-1}. Following equilibration for 15 min, intra-arterial blood pressure was recorded for 10 min. In some animals, pharmacological studies were performed by intraperitoneal (I.P.) injections of the NOS inhibitor N^{ω}-nitro-L-arginine methyl ester hydrochloride (L-NAME, 100 mg kg^{-1}) or the adrenergic agonist phenylephrine (PE, 3 mg kg^{-1}).

Isometric tension vasomotor studies

Aortic vasomotor function was assessed using isometric tension studies in a wire myograph (Multi-Myograph 610M, Danish Myo Technology, Aarhus, Denmark). Mice were killed by cervical dislocation. Freshly harvested and cleaned thoracic aortas ($n = 5$–10 per group) were cut into two 2 mm aortic rings, which

were mounted in organ bath chambers containing 5 ml of Krebs–Henseleit buffer (KHB [in mmol l^{-1}]: NaCl, 120; KCl, 4.7; $MgSO_4$, 1.2; KH_2PO_4, 1.2; $CaCl_2$, 2.5; $NaHCO_3$, 25; and glucose, 5.5) at 37°C, gassed with 95% O_2–5% CO_2. All experiments were performed in the presence of 10 μM indomethacin to inhibit endogenous prostaglandin release. Rings were first allowed to equilibrate for 30 min and then gradually stretched to a passive tension of 15 mN. Rings were constricted with 60 mM KCl for 5 min to assess vessel viability. Dose–response contraction curves were performed using cumulative half-log concentrations of phenylephrine (10^{-9}–10^{-5} M). Vessels were then washed repeatedly with fresh KHB for 30 min, and then precontracted to approximately 90% of maximal tension with PE (typically 3×10^{-6} M). Dose–response relaxation curves for increasing cumulative concentrations of acetylcholine (ACh, 10^{-9}–10^{-5} M) were then established to assess endothelium-dependent relaxation mediated by endothelial NO release. Responses were expressed as a percentage of the precontracted tension. Vessels were washed and precontracted again to 90% maximal contraction with PE. N^{ω}-Nitro-L-arginine methyl ester (10^{-4} M; Sigma-Aldrich, UK) was then added to inhibit endogenous NO release from eNOS. Finally, the NO donor sodium nitroprusside (SNP, 10^{-10}–10^{-6} M) was added in increasing cumulative concentrations to test endothelium-independent smooth muscle relaxation in response to exogenous NO.

Measurement of NO production

Nitric oxide production was measured using an L-arginine to citruilline conversion assay in the presence of the specific arginase inhibitor *N*-hydroxy-nor-L-arginine (nor-NOHA), as previously described (de Bono *et al.* 2006). Aortas were opened longitudinally, and incubated in 250 μl of KHB containing 1 μM calcium ionophore and 5 μl of 1.85 MBq ml^{-1} ubiquitously labelled [^{14}C]L-arginine for 90 min at 37°C, prior to removing the supernatant. Endothelium lysis was induced by three cycles of freeze–thawing in 250 μl of water added to this supernatant. Sixty microlitres of 10% trichloroacetic acid was then added to deproteinate the samples, prior to centrifugation. Five hundred microlitres of this supernatant was then collected and added to 360 μl distilled water with 140 μl 10% trichloroacetic acid. Citruilline was resolved from arginine by HPLC, as previously described (de Bono *et al.* 2006), using a 250 mm × 4.6 mm Supelcosil LC-SCX 5 cation-exchange column (Sigma-Aldrich), a DG-980-50 degasser, two PU-2080 Plus pumps, a MX-2080-32 dynamic mixer (all from Jasco Ltd, Great Dunmow, UK) and a Lablogic β-RAM Model 3 continuous flow liquid scintillation detector (Lablogic Systems Ltd, Sheffield, UK). Products of arginine metabolism were eluted over 30 min using the following buffer (rate, 1 ml min^{-1}): 0–5 min 100% distilled water, 5–15 min linear gradient from 100% distilled water to 100% 200 mM sodium citrate (pH 3.0), and 15–30 min 100% sodium citrate (pH 3.0). Scintillant fluid (Lablogic) was mixed in-line at a ratio of 0.5:1.0 after elution from the column, before passage through the liquid scintillation detector. The integrals of citruilline peaks were expressed as a percentage of the total ^{14}C count.

Measurement of cyclic GMP levels

Cyclic GMP levels in aortas were measured as previously described (Ohashi *et al.* 1998). Mice were killed by cervical dislocation. Briefly, aortas ($n = 4$–7 per group) were opened longitudinally and pre-incubated in oxygenated Krebs–Hepes solution with 0.1 mmol l^{-1} 3-isobutyl-1-methylxanthine (IBMX; Sigma-Aldrich) at 37°C for 15 min and then stimulated with 1 μM acetylcholine for 3 min. Vessels were immediately snap-frozen in liquid nitrogen before homogenization in ice-cold 5% trichloroacetic acid containing 0.5 mM IBMX. Homogenates were centrifuged at 2000*g*, and trichloroacetic acid in the supernatant fractions was extracted with water-saturated ether. Cyclic GMP levels were measured in these fractions using a cGMP enzyme immunoassay kit (Cayman Chemical Co., Nottingham, UK), and results expressed as picomoles per milligram of trichloroacetic acid-precipitable protein solubilized with 1 M sodium hydroxide.

Statistics

Mean data for haemodynamic parameters, NO production and cGMP formation were analysed by one-way ANOVA with Bonferroni correction for repeated measures. For vasomotor studies, the mean responses of two arotic rings from each animal were combined to produce an n of 1. Dose–response curves from each group were compared using ANOVA for repeated measures followed by Bonferroni *post hoc* correction.

Results

Haemodynamic regulation in eNOS, GCH and eNOS/GCH transgenic mice

The haemodynamic findings by direct intra-arterial Millar® catheter measurements revealed no differences in systolic, mean or diastolic blood pressure between GCH-Tg and WT littermate mice. There was a significant reduction in systolic blood pressure in eNOS-Tg compared with their WT littermates ($P < 0.001$), with a non-significant trend towards a reduction in mean and diastolic pressure. This was reflected by a significant reduction

in pulse pressure in mice carrying the eNOS transgene ($P < 0.001$). However, the addition of the GCH transgene in eNOS/GCH double transgenic mice did not confer any additional effect on blood pressure when compared to eNOS-Tg alone. There were no significant differences in heart rate between the transgenic mice and their WT littermates (Fig. 1). This baseline haemodynamic phenotype was also confirmed by prior tail-cuff assessment in the same cohort (data not shown).

Non-selective systemic NOS inhibition by administration of 100 mg kg^{-1} intraperitoneal L-NAME caused a significant rise in blood pressure and a fall in heart rate in all animals (Fig. 2). The genotype-specific differences in systolic blood pressure at baseline were abolished by L-NAME, with a significantly greater rise in blood pressure in both eNOS-Tg and eNOS/GCH-Tg mice compared with WT littermates (for eNOS-Tg, systolic $P = 0.06$, mean $P < 0.05$, diastolic $P < 0.005$; for eNOS/GCH-Tg, systolic, mean and diastolic $P < 0.005$). There were no genotype-specific differences in the heart rate response to L-NAME (Fig. 2).

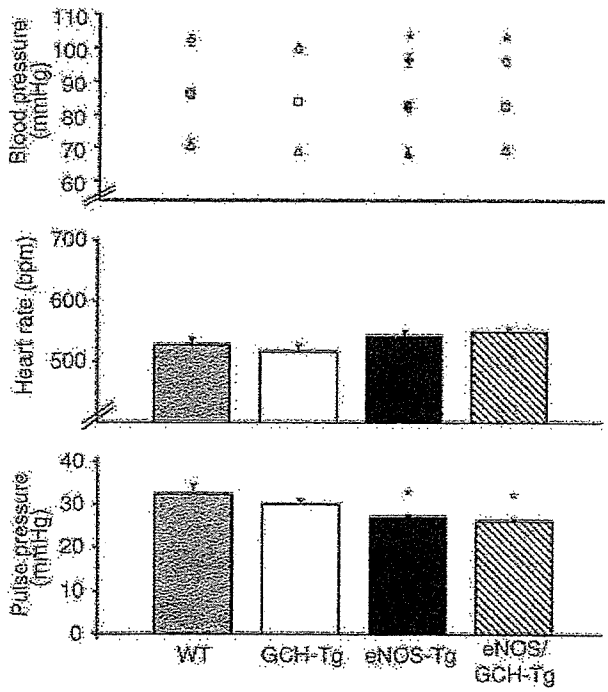

Figure 1. Invasive Millar® catheter haemodynamic measurements (systolic, diamonds; mean, squares; and diastolic, triangles) in $n = 7$–17 mice
There is a significant reduction in baseline systolic blood pressure in eNOS-Tg and eNOS/GCH-Tg animals compared with WT littermates (*$P < 0.01$). No significant difference in mean or diastolic blood pressure is shown by this technique. The proportionally greater effect on systolic blood pressure is reflected by a fall in pulse pressure in eNOS-Tg and eNOS/GCH-Tg animals (*$P < 0.01$) compared with WT littermates (means ± S.E.M.).

Adrenergic stimulation by administration of 3 mg kg^{-1} I.P. phenylephrine after NOS inhibition with L-NAME produced a significant rise in blood pressure and heart rate in WT and GCH-Tg mice, with no differences in the responses between these two groups (Fig. 2). Both eNOS-Tg and eNOS/GCH-Tg mice had a markedly reduced blood pressure response to phenylephrine compared to WT littermates ($P < 0.0005$). There were no differences in the heart rate response to I.P. phenylephrine between the genotype groups (Fig. 2).

Vasomotor function studies

We determined the functional significance of altering eNOS protein and BH4 bioavailability *in vitro* using isometric tension studies on a wire myograph (Fig. 3). The contractile responses to PE were unchanged in GCH-Tg mice, but were significantly reduced in aortic rings from both eNOS-Tg and eNOS/GCH-Tg mice compared with wild-type littermates. Endothelium-dependent relaxations in reponse to the receptor-mediated eNOS agonist ACh were unchanged in GCH-Tg mice but were significantly attenuated in eNOS-Tg mice compared with wild-type littermates. However, the presence of the GCH transgene on the eNOS-Tg background in eNOS/GCH-Tg animals had no effect, since relaxations in response to ACh were not different between eNOS-Tg and eNOS/GCH-Tg mice. Endothelium-independent relaxations in response to the NO donor SNP, unchanged in GCH-Tg mice, were significantly attenuated in both eNOS-Tg and eNOS/GCH-Tg mice, indicating a reduction

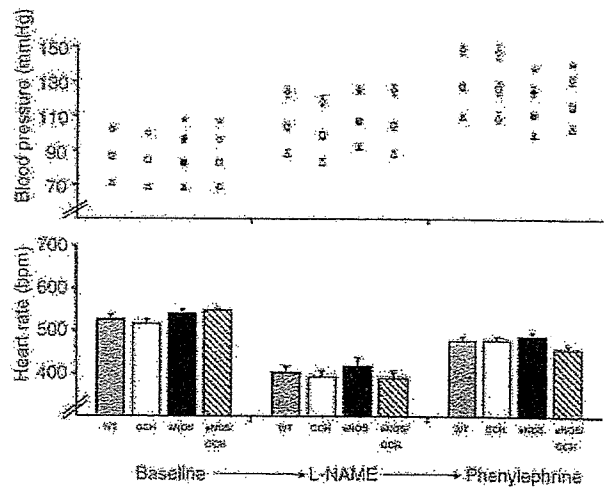

Figure 2. Intraperitoneal L-NAME (100 mg kg^{-1}) causes a rise in blood pressure and a fall in heart rate in all animals
This treatment abolished the baseline difference in blood pressure between genotype groups. Serial administration of 3 mg kg^{-1} I.P. phenylephrine following L-NAME caused a rise in heart rate in all animals. A rise in blood pressure was seen in WT and GCH-Tg animals but not in eNOS-Tg or eNOS/GCH-Tg littermates (*$P < 0.0001$; means ± S.E.M.).

in vascular smooth muscle responsiveness to NO (Fig. 3).

Vascular NO production

We examined the effect of endothelial eNOS and GCH overexpression on NO production from aortas by measurement of L-arginine to citruilline conversion in the presence of the specific arginase inhibitor *N*-hydroxy-nor-L-arginine (nor-NOHA). Citruilline production was markedly increased in the aortas of both eNOS-Tg and eNOS/GCH-Tg animals ($P < 0.0001$) compared with wild-type littermates. However, there was no further significant increase in NO production in eNOS/GCH-Tg aortas compared with eNOS-Tg alone (Fig. 4*B*).

Aortic cGMP formation

Since aortic relaxations in response to exogenous, as well as endothelium-derived, NO were significantly attenuated in eNOS-Tg and eNOS/GCH-Tg mice, we hypothesized that this may result from a desensitization in their downstream NO–cGMP pathway as a result of chronically enhanced NO production. In accordance with the vasomotor studies, aortic ACh-stimulated cGMP formation was found to be significantly reduced in both eNOS-Tg and eNOS/GCH-Tg mice compared with wild-type littermates (Fig. 4*A*).

Discussion

In this paper, we confirm that increased endothelial NO production in the eNOS-Tg mouse lowers blood pressure and paradoxically reduces vascular reactivity. We report for the first time the haemoydnamic phenotype of the GCH-Tg, a mouse model of endothelial BH4 augmentation, and the haemodynamic effect of increasing endothelial BH4 availability in the eNOS-Tg mouse by generating the eNOS/GCH double transgenic mouse. We show that the previously described changes in superoxide production between eNOS-Tg and eNOS/GCH-Tg mice, related to eNOS uncoupling, do not induce changes in blood pressure, suggesting that blood pressure regulation in these models may be more dependent on NO production than on superoxide production. Furthermore, we show that NO production rather than eNOS coupling by BH4 also appears to be the principal determinant of the cGMP pathway.

The importance of BH4 for the coupling of eNOS enzymatic activity to arginine oxidation and NO production is now well recognized (Vasquez-Vivar *et al.* 1998, 2003, 2004). In situations where BH4 is limiting, eNOS uncoupling results in increased superoxide production. This results in reduced bioavailability of NO both as a result of a reduction in NO production and as a result of increased NO scavenging by reactive oxygen species, leading to the production of peroxynitrite. We have previously shown that eNOS-Tg mice have increased aortic NO but also increased L-NAME-inhibitable superoxide production owing to uncoupling of eNOS as a result of a discordance between eNOS protein and its essential cofactor, BH4 (Bendall & Channon, 2005). This increase in aortic superoxide production was reversed by increasing vascular BH4 production in eNOS/GCH-Tg mice, which overexpress both endothelial eNOS and GTP cyclohydrolase 1 (the rate-limiting enzyme in endothelial BH4 synthesis; Bendall & Channon, 2005). In this study, we describe the effect of endothelial upregulation of eNOS and its cofactor BH4 on haemodynamic regulation in mice *in vivo* and compare it to measurements of vasomotor function *in vitro*.

Endothelium-specific eNOS-Tg mice were significantly hypotensive compared with WT littermates, a difference abolished by the NOS inhibitor L-NAME. This conforms with previously reported data from the same animal

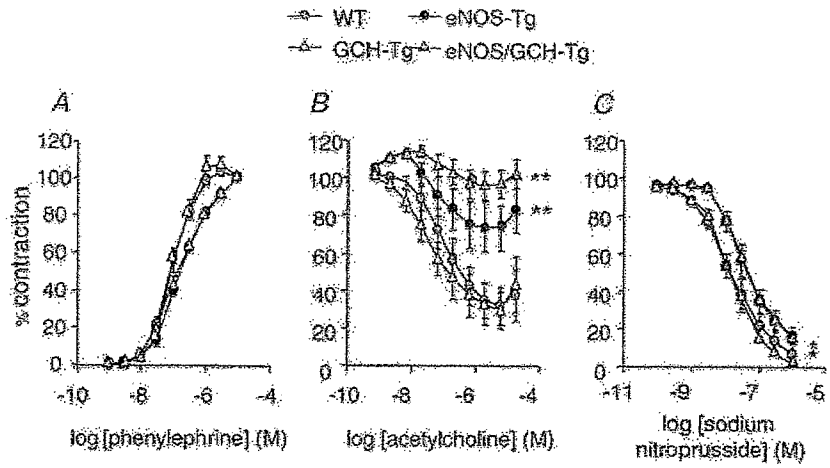

Figure 3. Isometric tension studies in aortic rings from WT, GCH-Tg, eNOS-Tg and eNOS/GCH-Tg mice ($n = 5$–10 animals per group) measured using a wire myograph
Dose–response curves for cumulative half-log concentrations of the α-adrenergic receptor agonist phenylephrine (*A*), the endothelium-dependent NO agonist acetylcholine (*B*) and the exogenous NO donor sodium nitroprusside (*C*). $^{*}P < 0.05$, $^{**}P < 0.01$ compared with wild-type measured using repeated measures ANOVA (means ± S.E.M.).

model (Ohashi *et al.* 1998). This finding is consistent with the expected effect of endothelial eNOS overexpression on enhanced endothelial NO production, leading to a reduction in smooth muscle tone and reduced blood pressure. It might be expected that this model would be associated with improved vascular responsiveness to activators of endothelial NO release, such as acetylcholine. However, we observed discordance between *in vivo* hypotension *versus* a significant impairment of endothelium-dependant relaxations *in vitro*, measured using wire myography. Furthermore, *in vitro*, aortic contraction in response to phenylephrine and relaxation in response to an exogenous NO donor (SNP) were found to be significantly impaired in eNOS-Tg and eNOS/GCH-Tg animals. This was reflected by an impaired pressor response to a phenylephrine bolus *in vivo*. These findings are consistent with those reported in the eNOS knockout mouse model, in which the opposite effect has been reported (Kojda *et al.* 2001), and suggest that chronic alterations in endothelial free radical signalling also have secondary effects on endothelium-independent vascular smooth muscle reactivity.

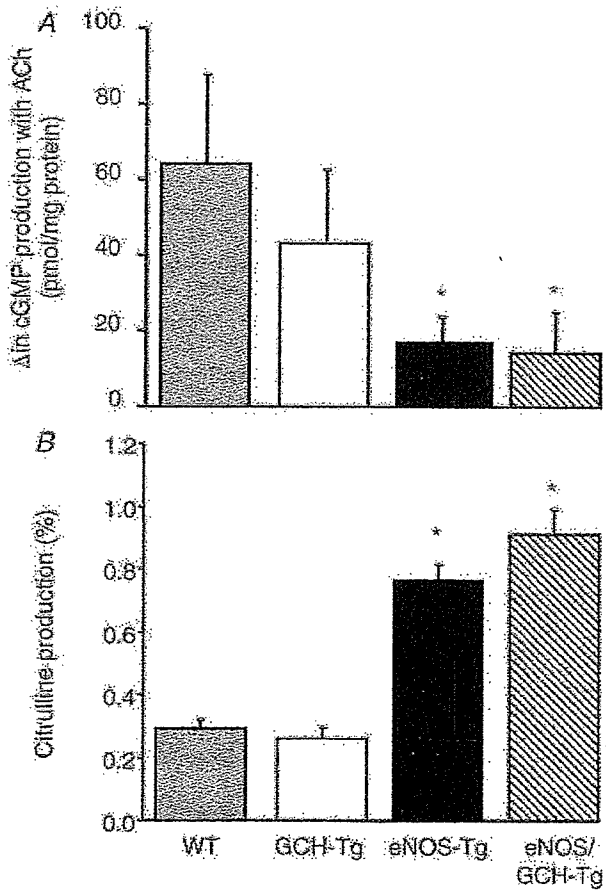

Figure 4. Cyclic GMP production and arginine to citruilline conversion in aortas
A, cyclic GMP levels after stimulation with 1 μmol l^{-1} acetylcholine for 3 min in the presence of 0.1 mmol l^{-1} IBMX at 37°C in aortas from wild-type, GCH-Tg, eNOS-Tg and eNOS/GCH-Tg mice ($n = 4$–7 animals per group). $^*P < 0.05$ compared with wild-type (means ± S.E.M.). *B*, NO production measured as L-arginine to citruilline conversion in $n = 8$–11 mice. There is a significant increase ($^*P < 0.0001$) in NO production in eNOS-Tg and eNOS/GCH-Tg animals compared with WT or GCH-Tg mice. There is no difference in aortic NO production between eNOS-Tg and eNOS/GCH-Tg animals (means ± S.E.M.).

The GCH-Tg mouse was normotensive and demonstrated no change in vasomotor function at myography compared with WT littermates. We have previously shown that the GCH-Tg preserves vasomotor function in the context of a disease model such as diabetes where it is otherwise impaired (Alp *et al.* 2003). The addition of the GCH transgene to eNOS-Tg mice in the eNOS/GCH-Tg animal had no additional effect on blood pressure compared with eNOS-Tg littermates. In accordance, vasorelaxations in response to endothelium-derived and exogenous NO were no different between eNOS/GCH-Tg and their eNOS-Tg littermates. This suggests that the known difference in superoxide production between the aortas of eNOS-Tg and eNOS/GCH-Tg animals is not an important determinant of blood pressure regulation or vascular tone. Rather, both blood pressure and vasomotor function appear to be more closely related to NO production, which is increased equally in both eNOS-Tg and eNOS/GCH-Tg mice.

Since aortic responses to exogenous as well as endothelium-dependent NO were attenuated in eNOS-Tg and eNOS/GCH-Tg mice, we hypothesized that this may result from downstream desensitization of their NO–cGMP signalling pathway as a result of chronic elevation of NO levels rather than owing to endothelial dysfunction. Acetylcholine-stimulated cGMP production was found to be significantly reduced in both eNOS-Tg and eNOS/GCH-Tg aortas, the two groups with attenuated vasorelaxations to ACh and SNP. It remains possible, however, that a component of the desensitization of the NO–cGMP pathway may result from a reduction in endothelial NO production in response to exogenous stimulation with ACh. Hence, whilst maximal NO production measured by arginine to citruilline conversion (in the presence of calcium ionophore) is increased in eNOS-Tg and eNOS/GCH-Tg aortas, it cannot be said with certainty that NO production in response to ACh is likewise increased.

There is therefore an apparent discordance between hypotension in mice expressing the eNOS transgene and vascular hyporeactivity, although both appear to be mediated directly or indirectly by increased NO production and are independent of superoxide. One explanation might be that the mechanisms which regulate the set-point of vascular tone and therefore blood pressure